Article

Search for Improved Host Architectures: Application of de Novo Structure-Based Design and High-Throughput Screening Methods To Identify Optimal Building Blocks for Multidentate Ethers

Benjamin P. Hay, Alexander A. Oliferenko, Jamal Uddin, Cungen Zhang, and Timothy K. Firman

J. Am. Chem. Soc., **2005**, 127 (48), 17043-17053• DOI: 10.1021/ja055169x • Publication Date (Web): 02 November 2005

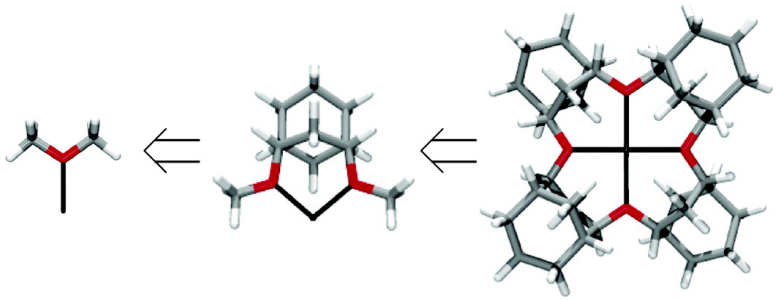

J|A|C|S
ARTICLES
Published on Web 11/02/2005

Search for Improved Host Architectures: Application of de Novo Structure-Based Design and High-Throughput Screening Methods To Identify Optimal Building Blocks for Multidentate Ethers

Benjamin P. Hay,* Alexander A. Oliferenko, Jamal Uddin, Cungen Zhang, and Timothy K. Firman

Contribution from the Chemical Sciences Division, Pacific Northwest National Laboratory, PO Box 999, Richland, Washington 99352

Received July 29, 2005; E-mail: ben.hay@pnl.gov

Abstract: This paper presents a computational approach to the deliberate design of improved host architectures. The approach, which involves the use of computer-aided design software, is illustrated by application to cation hosts containing multiple aliphatic ether oxygen binding sites. De novo molecule building software, HostDesigner, is interfaced with molecular mechanics software, GMMX, providing a tool for generating and screening millions of potential bidentate building block structures. Enhanced cation binding affinity can be achieved when highly organized building blocks are used to construct macrocyclic hosts.

Introduction

As illustrated in Figure 1, multidentate metal ion hosts can be viewed as assemblies of smaller structural elements, or building blocks, consisting of two donor atoms and the linkage that is used to connect them. For any given building block, the ability of the two donor atoms to achieve an optimal orientation with respect to the metal ion is dictated by structural constraints imposed by the linkage between them.[1] Because these structural constraints are an intrinsic property of the building block architecture, the same structural constraints are also present, to a large extent, in multidentate hosts that contain the building block. As a result, changes in metal ion binding affinity brought about by modifications to larger host structures can often be predicted on the basis of the behavior of simple building block analogues.

For example, a general rule of host design is that replacing an ethylene-bridged amine building block with a propylene-bridged amine building block results in increased selectivity for smaller metal ions.[2] This behavior, which has been observed with both podands and macrocycles, is explained by the differing metal size preferences exhibited by the analogues 1,2-ethylenediamine and 1,3-propylenediamine.[1,3] Similarly, it has been shown that changes in metal ion binding affinity caused by placing alkyl substitutents on 15-crown-5 and 18-crown-6 macrocycles can be quantitatively predicted by consideration of structural constraints present in alkylated dimethoxyethane analogues.[4]

The ethers shown in Figure 2 provide a clear example how structural constraints in a building block are preserved in a multidentate host. It has been established that the strongest interaction between an ether oxygen binding site and a group 1A or 2A cation occurs when the metal approaches along the ether dipole moment, yielding a trigonal planar oxygen atom.[5,6] This optimal orientation can be visualized by attaching a vector to the oxygen (Figure 2a). Dimethoxyethane, **1**, represents the simplest analogue of the ethylene-bridged ether building block. In the trans−gauche−trans binding conformation of **1**, the two ether dipole moments diverge (Figure 2b), illustrating that this structural element exhibits poor complementary for metal complexation.[6,7] In the D_{3d} binding conformation of 18-crown-

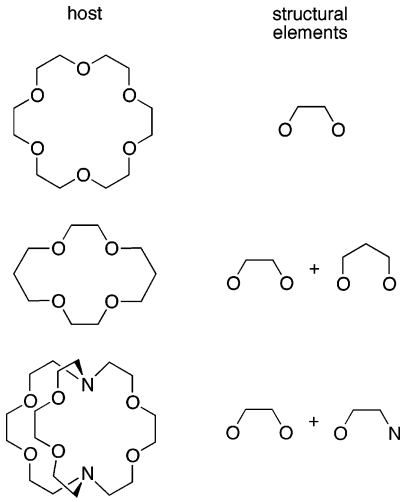

Figure 1. Multidentate hosts composed with groups of simple structural elements.

(1) Hay, B. P.; Hancock, R. D. *Coord. Chem. Rev.* **2001**, *212*, 61.
(2) Hancock, R. D.; Martell, A. E. *Chem. Rev.* **1989**, *89*, 1875.
(3) (a) Hancock, R. D. *Prog. Inorg. Chem.* **1989**, *37*, 187. (b) Hancock, R. D. *Acc. Chem. Res.* **1990**, *23*, 253.
(4) Hay, B. P.; Zhang, D.; Rustad, J. R. *Inorg. Chem.* **1996**, *35*, 2650.
(5) Hay, B. P.; Rustad, J. R.; Hostetler, C. J. *J. Am. Chem. Soc.* **1993**, *115*, 11158.
(6) Hay, B. P.; Rustad, J. R. *J. Am. Chem. Soc.* **1994**, *116*, 6316.
(7) Hay, B. P.; Rustad, J. R. *Supramol. Chem.* **1996**, *6*, 383.

10.1021/ja055169x CCC: $30.25

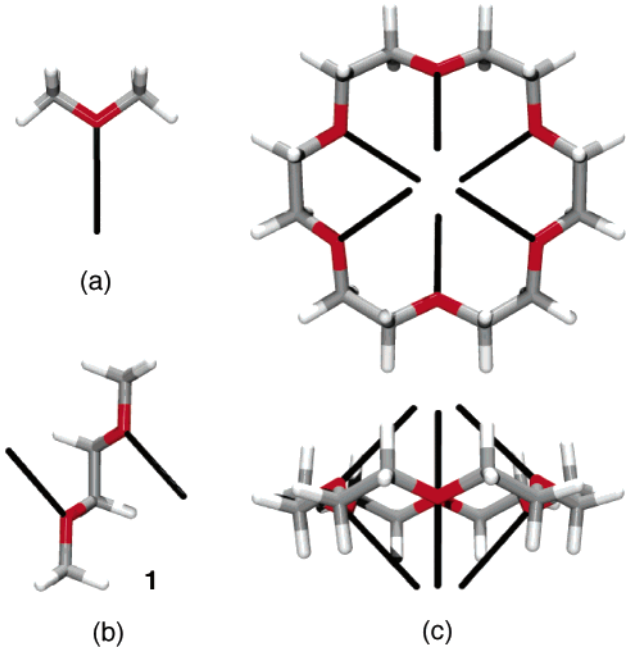

Figure 2. MM3-optimized geometries of (a) dimethyl ether (DME), (b) trans-gauche−trans conformation of dimethoxyethane, and (c) D_{3d} conformation of 18-crown-6. Vectors attached to each oxygen atom depict the dipole moment for each ether group; in other words, they illustrate the optimal cation location with respect to each oxygen atom.

6, which is most prevalent conformation observed for K^+ complexes, each $-CH_2OCH_2CH_2OCH_2-$ group exhibits the same trans−gauche−trans conformation. A dipole orientation identical to that in **1** is observed for each building block resulting in three dipoles that converge above and three dipoles that converge below the center of the cavity (Figure 2c).[1] Thus, although 18-crown-6 has a good cavity size for K^+, this architecture fails to provide a complementary dipole orientation. As a result, the K^+ binding affinity is less than could be achieved with a host in which all six aliphatic ether binding sites were arranged to provide both optimal cavity size and dipole orientation.

In theory, there is a maximum binding affinity that can be attained when a given set of binding sites are assembled about a specific metal ion. This theoretical limit, which is moderated by a variety of environmental factors including the solvent, counterions, ionic strength, temperature, etc., will be reached only when the building blocks used to construct the multidentate host are themselves structurally organized for metal ion complexation.[8] A high degree of structural organization is obtained when two conditions are met. First, the building block must be able to adopt a conformation in which all binding sites are positioned to structurally complement the metal ion.[1] Second, the building block should exhibit a limited number of stable conformations and the binding conformation should be low in energy relative to other possible forms.[9] Dramatic enhancements in binding affinity can be obtained when these two criteria are achieved.[10]

The ethylene-linked ether building block, $-OCH_2CH_2O-$, which is the defining structural element of simple crown ether macrocycles, fails to meet these criteria. There have been many attempts to modify the performance of multidentate ether hosts by replacing the ethylene linkages with other structures.[11] The choice of replacement building blocks has been, for the most part, motivated by the desire either to alter the size of the host cavity or to restrict conformational freedom. Little attention, however, has been given to the influence of the linking architecture on the orientation of the ether dipole moments.

Optimal building blocks for multidentate aliphatic ether hosts must have stable conformations that allow the two dipole moment vectors to converge at the metal ion. Identification of linkage architectures that exhibit this geometric property is not a trivial task. Until recently, this enterprise would have involved the evaluation of trial structures generated by hand with a graphical user interface, an extremely time-consuming process. To address the problem of how to locate host building blocks that are organized for guest complexation, we have adopted computational approaches pioneered by the pharmaceutical industry.[12]

We have developed de novo structure-based design software, HostDesigner (HD), specifically tailored to discover host architectures for small guest molecules.[13,14] HD generates and evaluates millions of candidate structures in minutes on a desktop personal computer and rapidly identifies three-dimensional architectures that position binding sites to provide a user-specified geometry with respect to the guest. The molecule-building algorithms combine input host−guest fragments with linking fragments taken from a large database. When using these fragments to build molecules, all possible connectivities, stereochemistries, and conformations are constructed, which yields large numbers of structures. These structures are scored on the basis of geometric factors, and a list of the top candidates is output. The initial screening performed by HD can be improved by subjecting the top candidates to more accurate, but slower, screening methods that are based on strain energies obtained with molecular mechanics calculations.[4−6,15]

In a systematic computational study, we have applied these methods to search for linkages that would provide architecturally

(8) (a) Steed, J. W.; Atwood, J. L. *Supramolecular Chemistry*; John Wiley & Sons Ltd.: Chichester, U.K., 2000. (b) Schneider, H.-J.; Yatsimirski, A. K. *Principles and Methods in Supramolecular Chemistry*; John Wiley & Sons Ltd.: Chichester, U.K., 2000.

(9) (a) Busch, D. H.; Farmery, K.; Goedken, V.; Katovic, V.; Melnyk, A. C.; Sperati, C. R.; Tokel, N. *Adv. Chem. Ser.* **1971**, *No. 100*, 44. (b) McDougall, G. J.; Hancock, R. D.; Boeyens, J. C. A. *J. Chem. Soc., Dalton Trans.* **1978**, 1438. (c) Anicini, A.; Fabbrizzi, L.; Paoletti, P.; Clay, R. M. *J. Chem. Soc., Dalton Trans.* **1978**, 577. (d) Cram, D. J.; Kaneda, T.; Helgeson, R. C.; Brown, S. B.; Knobler, C. B.; Maverick, E.; Trueblood, K. N. *J. Am. Chem. Soc.* **1985**, *107*, 3645. (e) Stack, T. D. P.; Hou, Z.; Raymond, K. N. *J. Am. Chem. Soc.* **1993**, *115*, 6466.

(10) Lumetta, G. J.; Rapko, B. M.; Garza, P. A.; Hay, B. P.; Gilbertson, R. E.; Weakley, T. J. R.; Hutchison, J. E. *J. Am. Chem. Soc.* **2002**, *124*, 5644.

(11) (a) Christensen, J. J.; Eatough, D. J.; Izatt, R. M. *Chem. Rev.* **1974**, *74*, 351. (b) Izatt, R. M.; Bradshaw, J. S.; Nielson, S. A.; Lamb, J. D.; Christensen, J. J. *Chem. Rev.* **1985**, *85*, 271. (c) Izatt, R. M.; Pawlak, K.; Bradshaw, J. S.; Bruening, R. L. *Chem. Rev.* **1991**, *91*, 1721. (d) An, H.; Bradshaw, J. S.; Izatt, R. M. *Chem. Rev.* **1992**, *92*, 543. (e) Izatt, R. M.; Pawlak, K.; Bradshaw, J. S. *Chem. Rev.* **1995**, *95*, 2529. (f) Walkowiak, W.; Charewicz, W. A.; Kang, S. I.; Yang, I.-W.; Pubia, M. J.; Bartsch, R. A. *Anal. Chem.* **1990**, *62*, 2018. (g) Walkowiak, W.; Kang, S. I.; Stewart, L. E.; Ndip, G.; Bartsch, R. A. *Anal. Chem.* **1990**, *62*, 2022. (h) Steed, J. W. *Coord. Chem. Rev.* **2001**, *215*, 171. (i) Gokel, G. W.; Leevy, W. M.; Weber, M. E. *Chem. Rev.* **2004**, *104*, 2723.

(12) (a) Kuntz, I. D.; Meng, E. C.; Shoichet, B. K. *Acc. Chem. Res.* **1994**, *27*, 117. (b) Lybrand, T. P. *Curr. Opin. Struct. Biol.* **1995**, *5*, 224. (c) Böhm, H.-J. *Prog. Biophys. Mol. Biol.* **1996**, *66*, 197. (d) Murcko, A.; Murcko, M. A. *J. Med. Chem.* **1995**, *38*, 4953. (e) Eldridge, M. D.; Murray, C. W.; Auton, T. R.; Paolini, G. V.; Mee, R. P. *J. Comput.-Aided Mol. Des.* **1997**, *11*, 425. (f) Kitchen, D. B.; Decornez, H.; Furr, J. R.; Bajorath, J. *Nat. Rev.* **2004**, *3*, 935.

(13) Hay, B. P.; Firman, T. K. *Inorg. Chem.* **2002**, *41*, 5502.

(14) (a) Hay, B. P.; Firman, T. K. *HostDesigner User's Manual*; PNNL-13850; Pacific Northwest National Laboratory: Richland, WA, 2004. (b) HostDesigner software and User's Manual are available free of charge via the Internet at http://hostdesigner.emsl.pnl.gov.

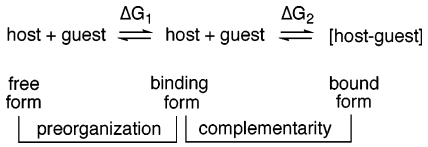

Figure 3. Irrespective of the actual complexation mechanism, the structural reorganization in the host that occurs upon binding the guest viewed as taking place in two steps defining three distinct structural states for the host: bound form, binding form, and free form.[4] The bound form is the structure of the host when complexed with the guest, the binding form is the host conformation obtained after removing the guest and optimizing the host, and the free form is the global minimum conformation of the host.

superior aliphatic ether building blocks. Herein we present the details of this study, including strategies for defining host−guest fragments and controlling the selection of linking fragments used to assemble them. The best building block candidates are reported, and examples are given to illustrate how these candidates could be employed to produce highly organized host architectures.

Methods

Structure Generation. Bidentate aliphatic ether building block candidates were constructed using the de novo structure-based design software, HostDesigner (HD).[13,14] This software assembles host structures by connecting molecular fragments. In each of the five types of runs conducted in this study, two aliphatic ether−metal fragments were connected with hydrocarbon linkages taken from the default HD fragment database. As will be described in the Results and Discussion, information needed to create the ether−metal fragments was obtained from molecular mechanics potential surfaces and geometric data taken from the Cambridge Structural Database.[16] Input files for all runs are provided as Supporting Information.

Scoring Methods. HD outputs an ASCII file containing Cartesian coordinates for a series of host structures presented in order of decreasing complementarity for the guest. The initial evaluation of complementarity is based on geometric factors.[13] During the construction of the ether−metal complex fragments, each metal ion was positioned to have the strongest interaction with the ether oxygen donor atom, in other words, to give the most complementary geometry. When HD builds a structure by combining two complex fragments with a linking fragment, the distance between the two metal ions provides a simple criterion for the rapid evaluation of the degree of complementarity offered by the host. Although approximate in nature, the geometry-based scoring method used by HD provides a rapid means for selecting the best candidates from a large group of potential structures.

Subsequent molecular mechanics analyses were applied to provide a more accurate prioritization of the top candidates. The evaluation is based on the well established use of molecular mechanics strain energies that are associated with the structural reorganization of the host upon guest complexation.[4−6,15] It is convenient to partition the structural reorganization into a two-step process as shown in Figure 3. In the first step, the host goes from the free form, defined as the lowest energy conformation of the host, to the binding form. The difference in steric energy between these two forms, ΔU_1, is a measure of the degree of preorganization. In the second step, the host goes from the binding form to the bound form. The difference in steric energy between these two forms, ΔU_2, is a measure of the degree of complementarity offered by the binding conformation.

An interface between HD and GMMX[17] was developed to automate the molecular mechanics evaluations. These evaluations occur in two steps. In the first step, ΔU_2 values are calculated for the top 5000 candidates. The ΔU_2 values can be used to estimate the free energy change ΔG_2 (see Figure 3), if it is assumed that (a) the calculated form of the complex represents the most populated form, (b) in the absence of strain, the intrinsic bond strength, $\Delta H_{2,\mathrm{int}}$, is constant for a constant set of M−L interactions, and (c) entropic contributions are constant except for restricted bond rotation associated with the formation of the host−guest complex. The magnitude of the latter term given by the empirical relationship, $0.31N_{\mathrm{rot}}$ kcal mol^{-1}, where N_{rot} is the number of freely rotating bonds restricted on complexation.[18] Thus, ΔG_2 values in kcal mol^{-1} are provided by eq 1, consisting of an enthalpic component, ΔU_2, and entropic component, $0.31N_{\mathrm{rot}}$, and some constant contribution a. The HD program applies a group additivity approach to obtain an approximate value for the free energy change ΔG_1(est).[14a] If one ignores the constant term, eq 2 gives a value for the relative binding free energy, ΔG_{rel}. The top 5000 candidates are then placed in order of increasing ΔG_{rel} values. All ΔG_{rel} values will be ≥ 0 kcal mol^{-1}, with the best possible $\Delta G_{\mathrm{rel}} = 0$, obtained when $\Delta U_2 = 0$ (complementary), $N_{\mathrm{rot}} = 0$ (no restricted rotations), and ΔG_1(est) $= 0$ (preorganized).

$$\Delta G_2 = \Delta H_{2,\mathrm{int}} + \Delta U_2 + T\Delta S_2 = \Delta U_2 + 0.31N_{\mathrm{rot}} + a \quad (1)$$

$$\Delta G_{\mathrm{rel}} = \Delta G_1(\mathrm{est}) + \Delta U_2 + 0.31N_{\mathrm{rot}} \quad (2)$$

In the second step, conformational analyses are performed on the top 500 host structures from the first step to obtain values for ΔU_1. The ΔU_1 values yield an improved estimate for ΔG_1 if it is assumed that (a) in the absence of the guest the majority of the host is in the global minimum conformer and (b) entropic contributions are constant. Thus, ΔG_1 values are provided by eq 3, consisting of an enthalpic component, ΔU_1, and some constant contribution b. As in the first step, if one ignores the constant terms, combining eq 1 and 3 yields eq 4, which gives an improved value for the relative binding free energy, ΔG_{rel}. The top 500 candidates are then placed in order of increasing ΔG_{rel} values to yield the final candidate ranking. Like before, ΔG_{rel} values will be ≥ 0 kcal mol^{-1}, with 0 representing the best possible score.

$$\Delta G_1 = \Delta U_1 + T\Delta S_1 = \Delta U_1 + b \quad (3)$$

$$\Delta G_{\mathrm{rel}} = \Delta U_1 + \Delta U_2 + 0.31N_{\mathrm{rot}} \quad (4)$$

Molecular Mechanics Calculations. Molecular mechanics calculations were performed with the MM3 force field[19] as implemented in GMMX,[17] a program that is capable of performing both geometry optimizations and conformational analyses. The default MM3 parameter set was extended to include metal−ether interactions. Metal-dependent parameters for divalent metal ions of differing size were interpolated from a prior MM3 parametrization for complexes of aliphatic ethers with the group 1A and 2A cations.[6]

(15) (a) Hay, B. P. In *Metal-Ion Separation and Preconcentration, Progress and Opportunities*; ACS Symposium Series 716; Bond, A. H., Dietz, M. L., Rogers, R. D., Eds.; American Chemical Society: Washington, DC, 1999; pp 102−113. (b) Hay, B. P. In *Metal Separation Technologies Beyond 2000: Integrating Novel Chemistry with Processing*; Liddell, K. C., Chaiko, D. J., Eds.; Minerals, Metals, Materials Society: Warrendale, PA, 1999; pp 3−13. (c) Sachleben, R. A.; Moyer, B. A. In *Metal-Ion Separation and Preconcentration, Progress and Opportunities*; ACS Symposium Series 716; Bond, A. H., Dietz, M. L., Rogers, R. D., Eds.; American Chemical Society: Washington, DC, 1999; pp 114−132. (d) Bond, A. H.; Chiarizia, R.; Huber, V. J.; Dietz, M. L.; Herlinger, A. W.; Hay, B. P. *Anal. Chem.* **1999**, *71*, 2757. (e) Dietz, M. L.; Bond, A. H.; Hay, B. P.; Chiarizia, R.; Huber, V. J.; Herlinger, A. W. *Chem. Commun.* **1999**, *13*, 1177. (f) Hay, B. P.; Dixon, D. A.; Vargas, R.; Garza, J.; Raymond, K. N. *Inorg. Chem.* **2001**, *40*, 3922.

(16) Allen, F. H. *Acta Crystallogr.* **2002**, *B58*, 380.

(17) The GMMX program, a component of PCModel, is available through Dr. Kevin Gilbert, Serena Software, Box 3076, Bloomington, IN 47402.

(18) (a) Eblinger, F.; Schneider, H.-J. *Angew. Chem., Int. Ed.* **1998**, *37*, 826. (b) Mammen, M.; Shakhnovich, E. I.; Whitesides, G. M. *J. Org. Chem.* **1998**, *63*, 3168. (c) Houk, K. N.; Leach, A. G.; Kim, S. P.; Zhang, X. *Angew. Chem., Int. Ed.* **2003**, *42*, 4872. (d) Deanda, F.; Smith, K. M.; Liu, J.; Pearlman, R. S. *Mol. Pharmacol.* **2004**, *1*, 23.

(19) Allinger, N. L.; Yeh, Y. H.; Lii, J.-H. *J. Am. Chem. Soc.* **1989**, *111*, 8551.

Because there are two metals present in the structures created by HD, a procedure was required to generate input geometries for the host−guest complex that were used in the determination of ΔU_1. The process is as follows. A single metal is placed at the average coordinates of the original two metals, and the original two are removed. The resulting structure was optimized to obtain U(complex). Input coordinates for the determination of U(host, binding form) were obtained by removing the metal from the optimized complex. After optimization, the binding conformation of the host provided input coordinates for conformational analysis.

Conformational searches were performed with default GMMX control parameters. During the searches, trial structures were generated by alternating between the "bonds method" and the "Cartesian method". In the "bonds method", trial structures are generated by randomly rotating a subset of bonds. In the "Cartesian method", trial structures are generated by removing hydrogen atoms, randomly moving the remaining atoms, and replacing the hydrogen atoms. A search was terminated when one of the stopping criteria is met, either exceeding a total of 100 000 trials or after 50 consecutive trials in which no new conformation is located within 3.5 kcal mol^{-1} of the global minimum.

Electronic Structure Calculations. Geometries of macrocyclic hosts and their cation complexes were optimized at the RHF/6-31G* level of theory with the NWChem program.[20] The electronic binding energy, ΔE_2, was obtained as the energy of the host−guest complex minus the energy of the host binding conformation minus the energy of the guest.

Hardware. HD and GMMX calculations were performed on a MacIntosh G5 computer with a 2 GHz PowerPC 970 processor. RHF calculations were performed on a massively parallel HP/Linux Itanium-2 cluster.

Results and Discussion

Metal−Ether Fragments. As implied by the term "structure-based design", the host architectures that are assembled by HD are both built and evaluated on the basis of prior knowledge of molecular structure. In this application, diether hosts are assembled by linking three fragments. These are two host−guest fragments that will be connected with a hydrocarbon fragment taken from a database. The hydrocarbon fragments are based on MM3-optimized geometries. With one exception, which occurs when the two input fragments are connected directly to one another, connecting the fragments leads to the formation of two single bonds. Both the bond lengths and the dihedral angles assigned to these two bonds are based on predetermined MM3 potential energy surfaces. In contrast, the geometry of the host−guest fragments is not predefined in HD and these data must be provided as input to the program.

The input file describing a host−guest fragment contains three pieces of information. These are the definition of the structure using Cartesian coordinates and a bond list, a list of hydrogen atoms that will be replaced by hydrocarbon fragments, and a specification of structural degrees of freedom within the host−guest fragment. When the host−guest fragment is constructed, the guest must be positioned relative to the host binding sites to define a complementary geometry, that is, a geometry that would give the strongest interaction between the binding sites and the guest. Dimethyl ether (DME) was selected as the host component for the initial HD run. After generation of the DME structure via MM3 geometry optimization, a metal ion was positioned along the dipole moment of the ether (vide supra). The M−O distance was set to 2.0 Å to complement a smaller cation such as Li^+ or Mg^{2+}. This process produced the host−guest structure shown in Figure 4a.

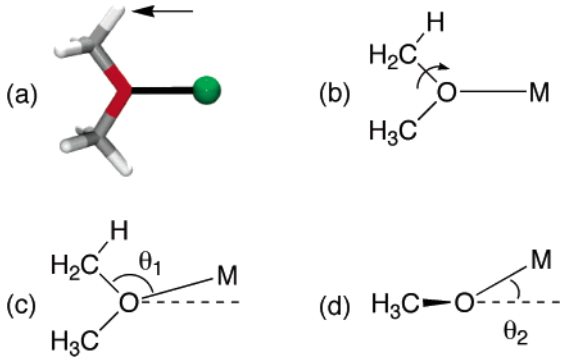

Figure 4. (a) Geometry of the DME−metal fragment where the arrow indicates the trans hydrogen atom to be replaced by a hydrocarbon linkage. The structural degrees of freedom scanned during the building process include (b) rotation of the CH_3 group to which the hydrocarbon linkage is attached, (c) the M−O−C angle, θ_1, and (d) the out-of-plane angle, θ_2.

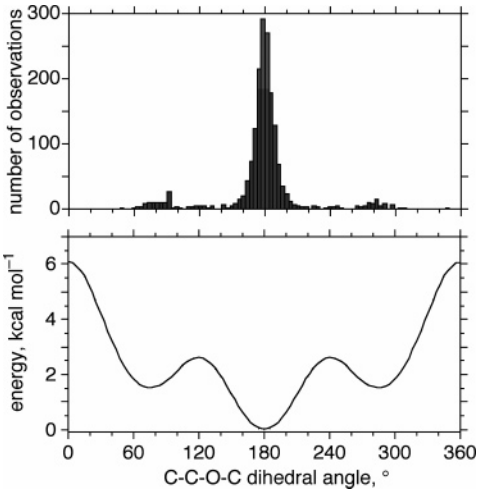

Figure 5. Comparison of the distribution of dihedral angles observed for rotation about the RCH_2O-CH_2R bond in primary ethers (top) versus the MM3 rotational potential surface for rotation about the $CH_3O-CH_2CH_3$ bond in methyl ethyl ether (bottom). The top plot represents 1799 examples extracted from the CSD with the following search constraints: $R_{fac} < 0.05$; no disorder; no errors.

The input file must also indicate which hydrogen atoms attached to the host can be replaced during the building process. There are three hydrogen atoms, designated gauche +, gauche −, and trans with respect to the C−O−C backbone, that could be replaced on a methyl carbon of DME. The choice of which hydrogen atom(s) to use was based on examination of calculated potential energy surfaces and crystal structure data.

Replacing any of hydrogen atoms of DME with a hydrocarbon substituent, R, will produce a primary alkyl group, CH_2R. In the simplest example, methyl ethyl ether is generated when a hydrogen atom is replaced with a methyl group. The MM3 potential surface for rotation about the $O-CH_2CH_3$ bond in methyl ethyl ether (Figure 5, bottom) reveals that it is the replacement of the trans hydrogen that yields the most stable conformation. This theoretical result is consistent with the distribution of dihedral angles about RCH_2O-CH_2R bonds observed in crystal structures, also showing a strong trans preference (Figure 5, top). Thus, to avoid assembling conformationally unstable structures, only the trans hydrogen was specified for replacement during the building process.

(20) Straatsma, T. P.; et al. *NWChem, A Computational Chemistry Package for Parallel Computers*, version 4.6; Pacific Northwest National Laboratory: Richland, WA 99352-0999, 2004.

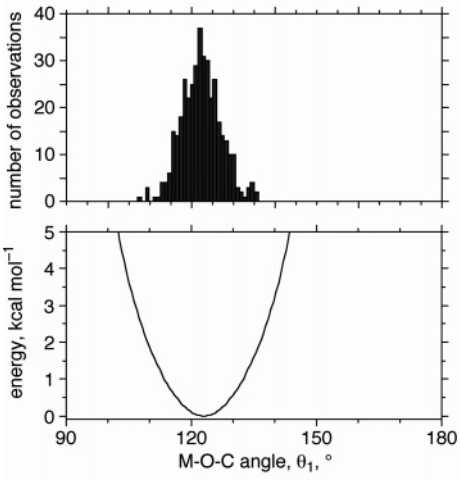

Figure 6. Comparison of the distribution of M−O−C angles for metal-coordinated diethyl ether ligands (top) versus the MM3 potential surface for in-plane M−O−C bending for $[Mg(DME)]^{2+}$ (bottom). The top plot represents 197 examples extracted from the CSD with the following search constraints: M−O distance ≤ 2.5 Å; R_{fac} < 0.05; no disorder; no errors.

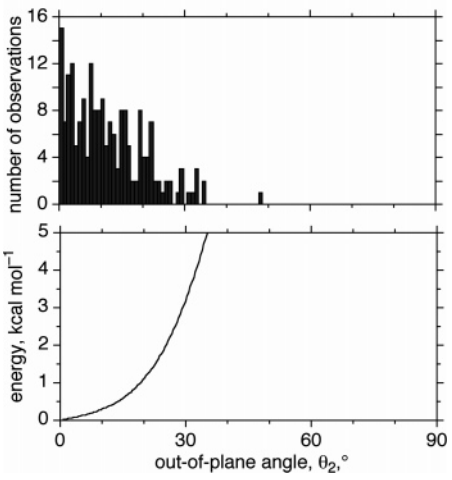

Figure 7. Comparison of the distribution of out-of-plane angles for metal-coordinated diethyl ether ligands (top) versus the MM3 potential surface for out-of-plane bending for $[Mg(DME)]^{2+}$ (bottom). The top plot represents 197 examples extracted from the CSD with the following search constraints: M−O distance ≤ 2.5 Å; R_{fac} < 0.05; no disorder; no errors.

Finally, the input file for a host−guest fragment can contain a specification of structural degrees of freedom, in other words, distances, angles, and dihedral angles, that can be varied during the building process.[14a] This feature takes into account known flexibility within the structure and allows HD to generate more hits of better quality. Three degrees of freedom were specified for the DME−metal fragment. These include rotation of the methyl group containing the hydrogen that will be replaced (Figure 4b) and bending of the M−O−C angle (Figure 4c) and out-of-plane angle (Figure 4d). As with the choice of which hydrogen(s) to replace, the settings for driving these structural features can be determined by examination of MM3 potential surfaces and/or behavior observed in crystal structures.

The extent of the variation in each degree of freedom was based on the displacement on potential energy surfaces that would result in a 1 kcal mol^{-1} rise in energy. For example, Figure 5 shows that this condition is achieved with C−O bond rotations of approximately ±30°. It can be seen that the bulk of the crystal structure data also falls within this range. Thus, this degree of freedom was varied from 150 to 210° in 10° increments.

Similar analyses were performed for the other two degrees of freedom. The potential surfaces for these distortions, computed using parameters for Mg^{2+}, are shown in Figures 6 and 7. The M−O−C angle θ_1, which has an equilibrium value of 123.5°, was allowed to vary ±10° in 10° increments. The out-of-plane angle θ_2, which has an equilibrium value of 0°, was allowed to vary ±20° in 10° increments.

The allowed flexibility is consistent with behavior observed in crystal structure examples of metal-coordinated unidentate ether ligands. To illustrate this Figures 6 and 7 show the distribution of θ_1 and θ_2 for diethyl ether ligands bound to any type of metal ion, including examples of group 1A and 2A metals, transition metals, and f-block metals. The mean M−O−C angle is 122 ± 4°, and the mean out-of-plane angle is 0 ± 14°. Corresponding values for a tetrahedral oxygen preference would be 109.5 and 54.7°, respectively. Thus, the experimental data are consistent with the potential energy surfaces and fully support a preferred trigonal planar geometry at the ether oxygen donor, regardless of the identity of the metal ion.

Initial Run: Connecting Two DME−Metal Fragments Using the Entire Linkage Database. The search for improved ether building blocks began with a HD run in which two DME−metal fragments (Figure 4a) were connected with hydrocarbon linkages. The linkage database used by HD contains over 10 000 structures composed of Csp^3, Csp^2, and H atoms. The fragments consist of all connectivities that can be made from 0 to 6 carbons, excluding three- and four-membered rings. The database also includes fragments made from all dimethylated five- and six-membered rings and selected bicyclic structures. Using all linkages within the database, HD constructed and evaluated a total of 143 985 540 geometries in under 7 min—a rate of more than 20 million geometries/min!

Molecular mechanics analyses were then used to obtain a more accurate ranking of the candidates. In the first step, ΔG_{rel} values (eq 2) were evaluated for the top 5000 candidates using metal-dependent parameters consistent with the M−O distance specified in the input fragment. Mg^{2+} parameters were used for the first set of runs (ideal Mg−O bond length, r_0 = 2.05 Å). This step was slower, taking 80 min to complete. In the final stage of scoring, conformational analyses were performed to obtain improved ΔG_{rel} values (eq 4). Because conformational analyses are more time-consuming, this last step is performed only on the top 500 candidates, taking 23 h to complete. Thus, from start to finish the total time spent to obtain the final result was 24 h and 27 min.

Top candidates from this run, **2**−**9**, are shown in Figure 8, and their scoring results are summarized in Table 1. These structures all have ΔG_{rel} values less than 3 kcal mol^{-1}, with **2** exhibiting the top score of 1.57 kcal mol^{-1}. For comparison, the ethylene-bridged architecture **1** (Figure 2) exhibits a ΔG_{rel} value of 6.77 kcal mol^{-1}. It is worth noting that although **1** was constructed during this run, it was ranked number 4200 after the first molecular mechanics evaluations and, therefore, was not retained in the final list of the best 500 candidates. This observation establishes that there are thousands of building blocks architectures that are better organized for metal ion binding than **1**.

This run was successful in that it located numerous architectures that are well organized for metal complexation.

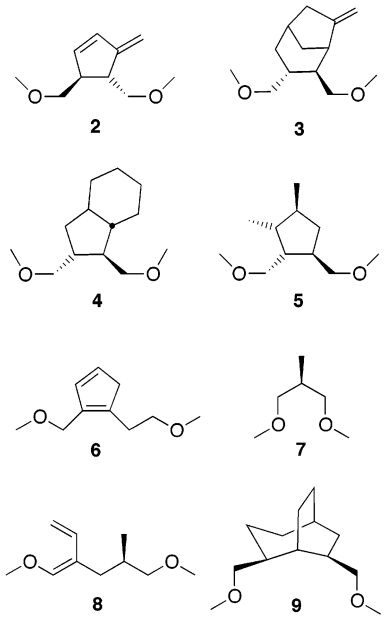

Figure 8. Top candidates obtained by connecting two DME−metal fragments using the entire linkage database. (See Table 1 for scoring data.)

Table 1. Scoring Data for Top Candidates Obtained by Connecting Two DME−Metal Fragments Using the Entire Linkage Database[a]

struct	ΔU_1	ΔU_2	$0.31N_{rot}$	ΔG_{rel}
2	0.13	0.20	1.24	1.57
3	0.00	0.44	1.24	1.68
4	0.91	0.23	1.24	2.38
5	1.03	0.23	1.24	2.50
6	0.72	0.38	1.55	2.64
7	1.54	0.10	1.24	2.87
8	0.79	0.54	1.55	2.88
9	0.43	1.28	1.24	2.95

[a] Values are given in kcal mol^{-1}. ΔG_{rel} values are obtained with eq 4.

However, inspection of **2**−**9** reveals an inherent problem with the de novo approach to molecule construction. When structures are indiscriminately assembled from molecular fragments, the process will produce numerous candidates that range from difficult to impossible to synthesize. Even if synthetic precursors containing linkages such as those shown in Figure 8 could be prepared, the majority of these structures possess properties that make them unattractive for use as building blocks for multidentate architectures.

With the exception of **7**, structures **2**−**9** are asymmetric. This property gives rise to the possibility of linkage isomerism when two or more building blocks are combined. With the exception of **6**, structures **2**−**9** are chiral. Combining chiral building blocks gives rise to the possible production of multiple stereoisomers. Both of these structural properties are undesirable in building blocks for multidentate hosts, ultimately leading to low synthetic yields and difficulties in isolating the desired product.

Another unattractive property is the size of the chelate rings that would be formed by structures such as **2**−**9**. With the exception of **7**, these structures all form ≥ seven-membered chelate rings with bite angles, in other words, O−M−O angles, exceeding 90°. Large bite angles are only suitable for guests with a coordination numbers ≤5. In addition, larger rings tend to lead to lower binding affinity, due to both adverse entropic and enthalpic factors.[2,18] In **2**−**9**, where N_{rot} values are ≥4, the entropy associated with restricted rotation makes a significant unfavorable contribution to ΔG_{rel}. In six out of these eight examples, this entropic contribution is the dominant term.

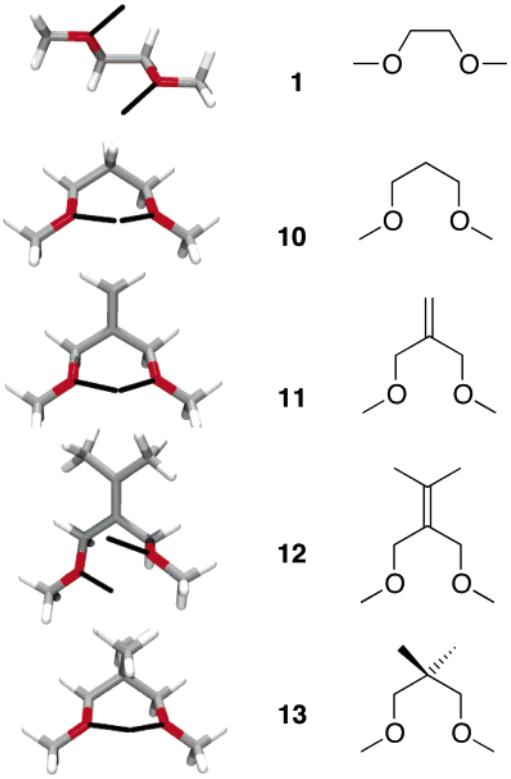

Figure 9. Binding conformations of the five candidates obtained by connecting two DME−metal fragments when severe restrictions are imposed on the selection of linkages. (See Table 2 for scoring data.) The 2.0 Å vectors attached to each oxygen atom depict the dipole moment for each ether group.

Connecting Two DME−Metal Fragments with a Highly Filtered Linkage Database. To address the concerns raised in the preceding section, several filters were added to HD to limit the linkages that are used during the building process. Filters can be used to discard all asymmetric, chiral, and prochiral linkages. In addition, the size of the chelate ring can be restricted to less than six by discarding all linkages that would place more than one carbon atom in the shortest path between the two DME−metal fragments. When these rather severe limitations are applied, combining two DME−metal fragments yields only the five structures, **1** and **10**−**13**, shown in Figure 9. Given their attractive synthetic attributes and small chelate ring sizes, it is not surprising to note that such simple structural elements have been widely exploited in multidentate ether hosts.[11]

The scoring data for these structures, Table 2, reveals that although these building blocks possess attractive synthetic properties, the degree of binding site organization is far from optimal. The ethylene bridged structure, **1**, formed by linking two DME-metal fragments directly to one another, is the only five-membered chelate ring that can be built from this input. While this structure is preorganized,[4] binding site orientation is poor, $\Delta U_2 = 5.8$ kcal mol^{-1}. In contrast, **10**−**13** are able to adopt binding conformations that are much more complementary, ΔU_2 values < 1.0 kcal mol^{-1}, but these structures are not preorganized and all exhibit alternate conformations that are significantly lower in energy. Finally, restricted rotation of the

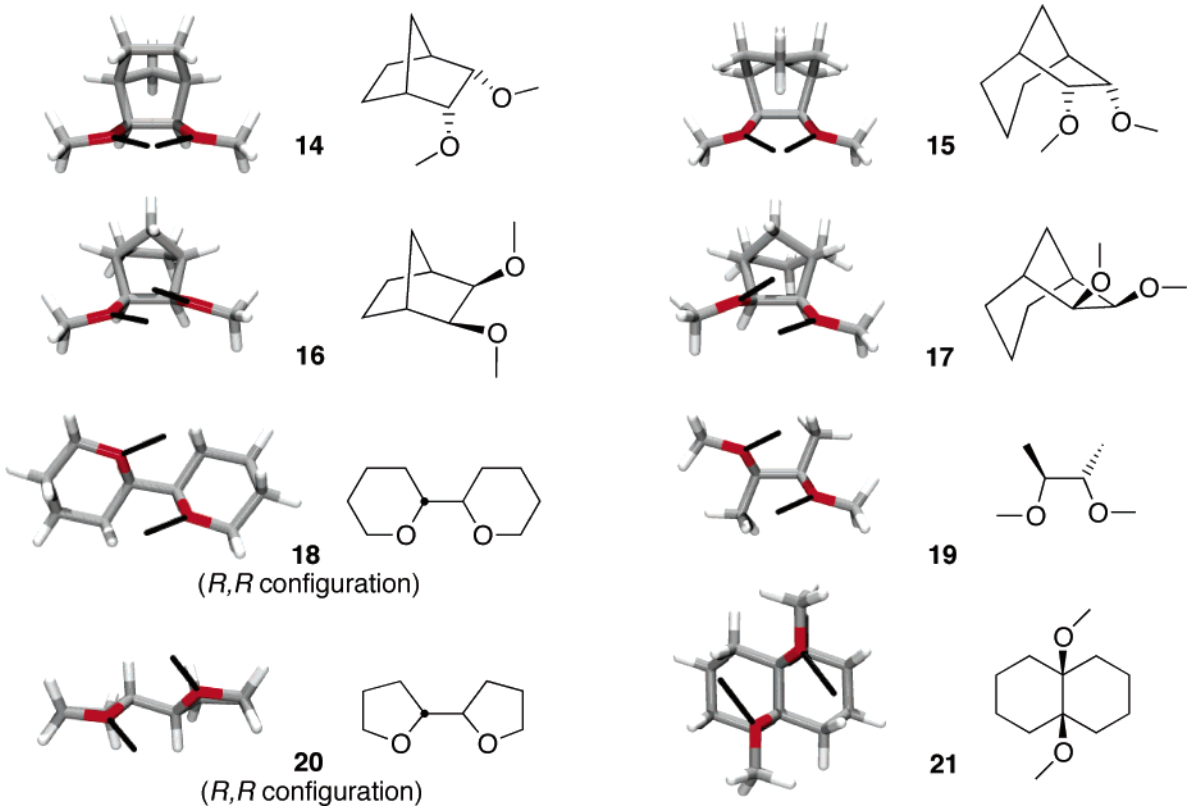

Figure 10. Binding conformations of top five-membered ring candidates obtained by connecting MeOH-, THF-, or THP-derived ether−metal fragments. (See Table 3 for scoring data.) The 2.0 Å vectors attached to each oxygen atom depict the dipole moment for each ether group.

Table 2. Scoring Data for the Five Candidates Obtained by Connecting Two DME−Metal Fragments with Severe Restrictions on Linkage Selection[a]

struct	ΔU_1	ΔU_2	$0.31N_{rot}$	ΔG_{rel}
10	1.81	0.11	1.24	3.17
11	1.86	0.19	1.24	3.28
12	1.29	0.97	1.24	3.50
13	1.92	0.67	1.24	3.83
1	0.00	5.84	0.93	6.77

[a] Values are given in kcal mol^{-1}. ΔG_{rel} values are obtained with eq 4.

three single bonds in **1** or the four single bonds in **10**−**13** provides additional adverse contributions to the ΔG_{rel} values.

Use of Additional Ether−Metal Fragments To Enhance Binding Site Organization. An obvious strategy to improve the degree of binding site organization is to reduce flexibility within the structure by reducing the number of rotatable bonds. This can be accomplished by incorporating rotatable bonds within ring structures. When the ring structures are composed of aliphatic carbons, this operation will always generate chiral centers. Thus, the advantage gained by rigidifying the building blocks will be paid for by the cost of increased synthetic difficulty when they are deployed.

One approach is to use cyclic ethers, such as tetrahydrofuran, THF, or tetrahydropyran, THP, to construct the ether−metal input fragments. When two of these fragments are combined, there will be two less rotatable bonds in the chelate ring. This gain in rigidity comes at the expense of introducing two chiral centers to the structure.

An alternate approach involves using methanol to construct an ether−metal input fragment. In this case, the O−H hydrogen is lost to form an O−C bond between the input fragment and a hydrocarbon linkage. The HD code, originally limited to form only C−C bonds, has been modified to include this capability. As with THF and THP input, two chiral centers are generated when two methoxy groups are attached directly to an aliphatic hydrocarbon ring system.

If one follows the same protocol used to create the DME−metal input fragments (vide supra), ether−metal input fragments were constructed from THF, THP, and MeOH molecules. Filters were applied to exclude use of linkages that (a) were asymmetric with respect to linkage isomerism and (b) would form large, > six-membered, chelate rings. With this input, three additional HD runs were performed, yielding new structures that could not be constructed from DME−metal fragments. The top results are summarized in Figures 10 and 11 and Table 3.

Building blocks that yield five-membered chelate rings are shown in Figure 10. These structures score significantly better, ≥2 kcal mol^{-1} lower, than **1**. The best structures, **14**−**17**, are formed by addition of two methoxy groups to bicyclic scaffolds. In the binding conformations of these structures, the O−C−C−O dihedral angles are ≤30°. These scaffolds offer a high degree of complementarity due to the fact that these dihedral angles go to 0° in the metal bound form, allowing the two ether dipole moments to achieve near convergence at the metal ion. Structures **18**−**21** do not exhibit this property, but with ΔU_2 values of ≤4.3 kcal mol^{-1}, all offer more complementary binding sites than **1**. Attaching two THP groups, **18**, or THF groups, **20**, directly to one another yields conformationally restricted building blocks with a single rotatable bond in the linkage between the ether groups. The only structure in this set that does not incorporate ring structures to restrict bond rotation,

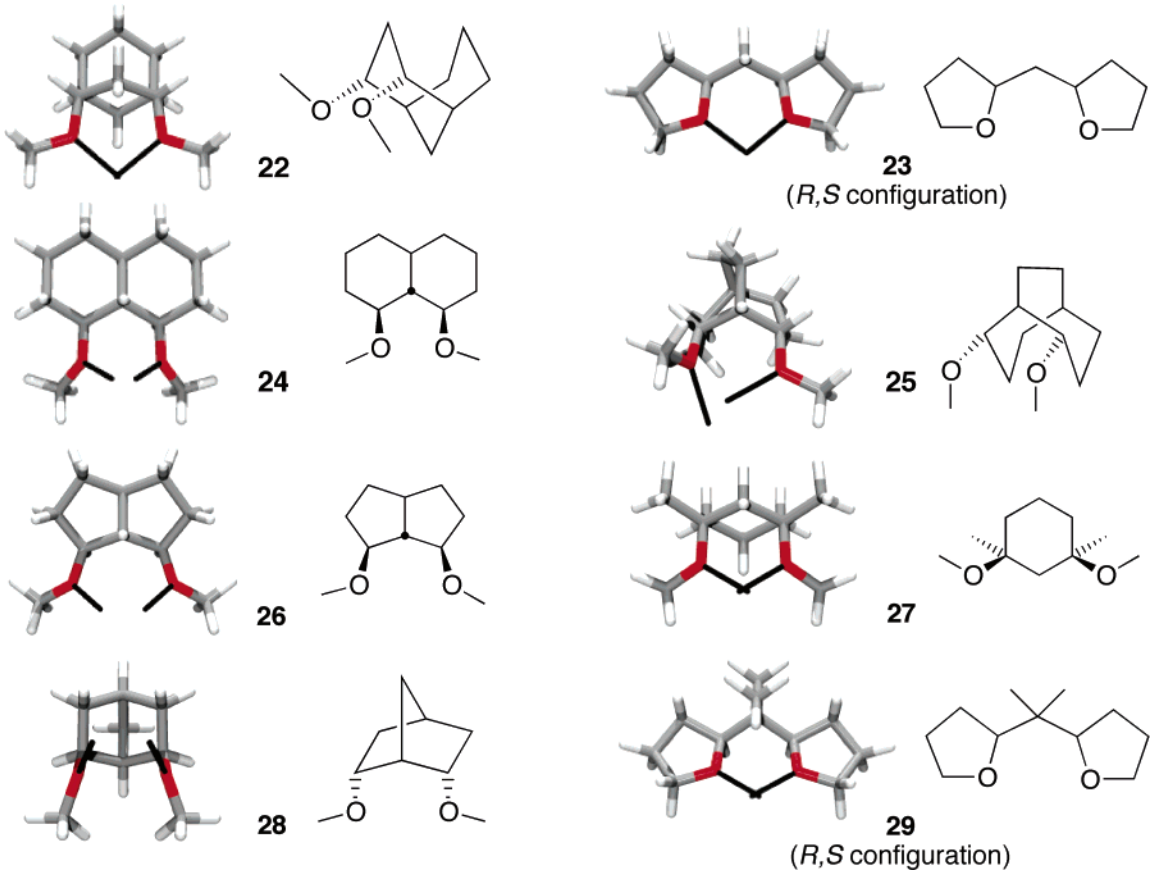

Figure 11. Binding conformations of top six-membered ring candidates obtained by connecting MeOH-, THF-, or THP-derived ether−metal fragments. (See Table 3 for scoring data.) The 2.0 Å vectors attached to each oxygen atom depict the dipole moment for each ether group.

Table 3. Scoring Data for Top Candidates Obtained Using Ether−Metal Fragments Derived from MeOH, THF, and THP[a]

struct	ΔU_1	ΔU_2	$0.31N_{rot}$	ΔG_{rel}
	Five-Membered Chelate Rings			
14	0.00	1.29	0.62	1.91
15	0.07	1.29	0.62	1.98
16	0.36	1.11	0.62	2.09
17	0.21	1.53	0.62	2.36
18	0.21	3.49	0.31	4.00
19	0.00	3.09	0.93	4.02
20	0.00	4.26	0.31	4.57
21	0.00	4.11	0.62	4.73
	Six-Membered Chelate Rings			
22	0.00	0.82	0.62	1.44
23	1.20	0.20	0.62	2.01
24	0.00	1.47	0.62	2.09
25	0.00	1.65	0.62	2.27
26	0.00	1.72	0.62	2.34
27	0.49	1.38	0.62	2.49
28	0.65	1.29	0.62	2.56
29	1.78	0.32	0.62	2.72

[a] Values are given in kcal mol^{-1}. ΔG_{rel} values are obtained with eq 4.

19, was previously identified as one of two cases where alkylation of **1** leads to a notable increase in cation complementarity.[4]

Building blocks that yield six-membered chelate rings are shown in Figure 11. These structures, formed either by the addition of two methoxy groups to bicyclic structures, **22** and **24**−**28**, or by linking two cyclic ethers, **23** and **29**, all have only two rotatable bonds in the connection between the ether oxygen atoms. Thus, they are all more rigid than **10**−**13**. The best structure in this set, **22**, has the overall lowest score obtained in all five runs, ΔG_{rel} = 1.44 kcal mol^{-1}. Structure **22** is preorganized (ΔU_1 = 0.00 kcal mol^{-1}), has only two rotatable bonds, and exhibits a fair degree of complementarity (ΔU_2 = 0.82 kcal mol^{-1}). Other preorganized structures in this set, **24**−**26** ($\Delta U_2 \geq$ 1.4 kcal mol^{-1}), are less complementary than **10**−**13** ($\Delta U_2 \leq$ 1.0 kcal mol^{-1}) but give a better overall score than the more flexible analogues.

Repeating the Searches with Longer M−O Distances. The building blocks presented up to this point were assembled with ether−metal input fragments in which the M−O distance was set to 2.0 Å. They were initially scored with respect to the degree that the ether dipole moments converged at a distance of 2.0 Å away from the ether oxygen atoms and subsequently scored, in part, with respect to the degree of strain within the host caused by binding to a small cation, Mg^{2+}. Further runs were performed to determine to what extent variation of M−O distance would impact the results.

The HD runs discussed above were repeated using ether−metal input fragments in which the M−O distance was set to either 2.5 or 3.0 Å. The molecular mechanics parameters that were used in the scoring for these runs were adjusted to correspond to a metal ion of the appropriate size. Although there were some shifts in the ordering of the candidates, the best building blocks from these runs were the same as those obtained when using the shorter 2.0 Å M−O distance.

The fact that the outcome was relatively insensitive to variation in M−O distance is explained on consideration of the terms that contribute to the score, ΔG_{rel} (eq 4). Two of the three terms are metal ion independent. Structures that score well

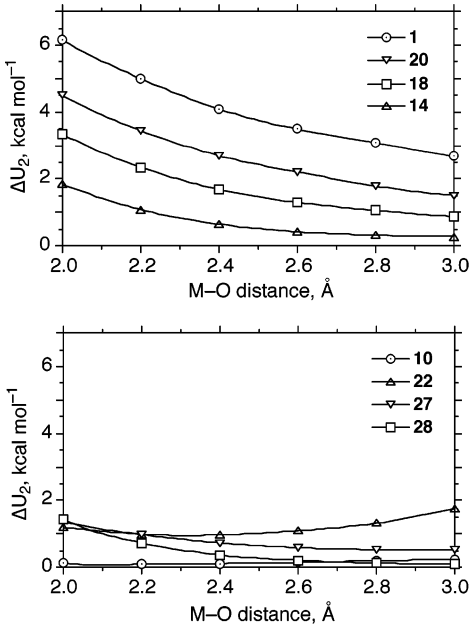

Figure 12. Plots of ΔU_2 versus M−O distance for five-membered chelate rings (top) and six-membered chelate rings (bottom).

because their binding conformation is energetically accessible (low ΔU_1 value) and they have a limited number of restricted rotations on chelation (low N_{rot} value) will do so regardless of the M−O distance. Thus, the only contribution to ΔG_{rel} that depends on the size of the metal ion is ΔU_2.

Plots of ΔU_2 versus M−O distance provide a convenient way to visualize the nature of this dependence.[7,21] Examples of such plots are presented in Figure 12. The five-membered chelate rings all show a monotonic decrease in strain on going from small to large metal ions. Thus, the relative ordering of ΔU_2 at different M−O distances is maintained. The six-membered rings exhibit two types of behavior, either a shallow minimum at smaller metal ion distances, as in **10** and **22**, or a monotonic decrease in strain on going from small to large metal ions, as in **27** and **28**. In contrast to the five-membered chelate rings, where the change in ΔU_2 values typically exceeds 2 kcal mol^{-1} on going from 2 to 3 Å, the ΔU_2 values for six-membered chelate rings are not as sensitive to M−O distance, typically changing by less than 1 kcal mol^{-1} over the same range.

Examples of Building Block Applications. The premise put forth in the Introduction was that the ubiquitous ethylene-bridged building block, **1**, does not provide a complementary architecture for metal ion complexation. Because the structural features that result in poor complementarity are present in multidentate hosts that contain this building block, such hosts also fail to provide complementary binding sites. As a result, they fail to reach the hypothetical binding affinity that could be achieved by an optimal architecture.

Application of de novo design methods has led to the identification of a number of building blocks (Figures 10 and 11) that exhibit higher degrees of binding site organization than **1**. When such building blocks are used to construct multidentate hosts, significant enhancements in binding affinity should be obtained. We now present three examples where this hypothesis is confirmed in silico. In each example, a poorly organized macrocyclic ether is compared with one constructed from

(21) Hancock, R. D.; McDougall, G. J. *J. Am. Chem. Soc.* **1980**, *102*, 6551.

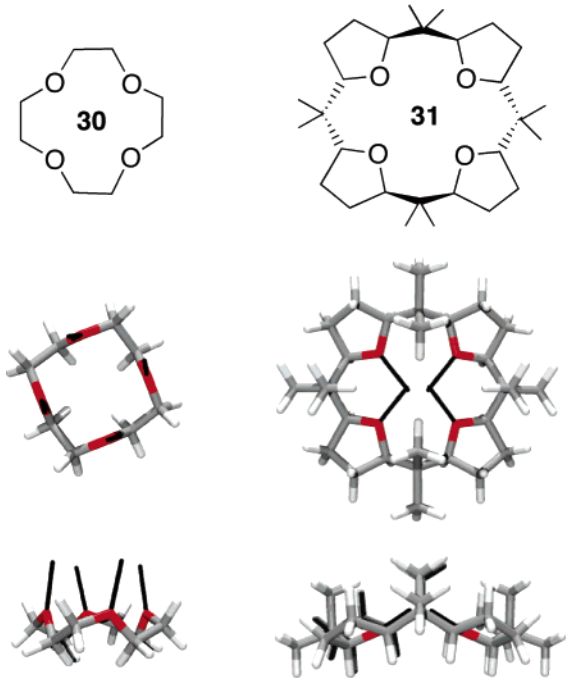

Figure 13. MM3-optimized geometries for the Li^+ binding conformations of **30** and **31**. The 2.0 Å vectors attached to each oxygen atom depict the dipole moment for each ether group.

improved building blocks identified in this study. Evaluation of the binding conformers for these macrocycles, both by visualization of ether dipole orientations and by ΔU_2 calculations, establish that the use of well-organized building blocks can lead to more effective host architectures. Enhanced cation binding affinities are confirmed by comparing electronic binding energies, ΔE_2, obtained at the RHF/6-31G* level of theory.

In the first example, we consider the complexation of Li^+ by 12-crown-4, **30**, and the known 16-crown-4 macrocycle, **31**, assembled from building block **22** (Figure 11). Although **30** ostensibly has a cavity size appropriate for Li^+, it binds only weakly to this cation[11] whereas **31** binds Li^+ strongly.[22] This reactivity difference is explained on consideration of the Li^+ binding conformations of **30** and **31**, taken from crystal structure data (Figure 13).[23,24] The ether dipoles in **30** are almost perpendicular to the cavity formed by the four oxygen atoms. In contrast, all four ether dipoles in **31** converge toward the center of the cavity, yielding a much more complementary binding site orientation. The effect of architectural differences in these two ligands is quantified with ΔU_2 values of 10.6 kcal mol^{-1} for **30** versus 1.2 kcal mol^{-1} for **31**, suggesting that **31** should exhibit a higher binding affinity. A substantial increase in Li^+ binding affinity is confirmed by ΔE_2 values of −103.1 kcal mol^{-1} for **30** versus −124.3 kcal mol^{-1} for **31**.

In the second example, we consider the complexation of Na^+ by 15-crown-5, **32**, and the theoretical 16-crown-4 mac-

(22) (a) Kobuke, Y.; Hanji, K.; Horiguchi, K.; Asada, M.; Nakayama, Y.; Furukawa, J. *J. Am. Chem. Soc.* **1976**, *98*, 7414. (b) Park, J. K. *J. Phys. Chem. A* **2002**, *106*, 3008.

(23) (a) Groth, P. *Acta Chem. Scand., Ser. A* **1981**, *35*, 463. (b) Power, P. P.; Xiaojie, X. *Chem. Commun.* **1984**, 358. (c) Bartlett, R. A.; Dias, H. V. R.; Hope, H.; Murray, B. D.; Olmstead, M. M.; Power, P. P. *J. Am. Chem. Soc.* **1986**, *108*, 6921. (d) Villacorta, G. M.; Rao, C. P.; Lippard, S. J. *J. Am. Chem. Soc.* **1988**, *110*, 3175. (e) Stenger, H.; Weller, F.; Dehnicke, K. *Z. Anorg. Allg. Chem.* **1991**, *606*, 109. (f) Emmerich, C.; Huttner, G. *J. Organomet. Chem.* **1993**, *81*, 447.

(24) Van Beylen, M.; Roland, B.; King, G. S. D.; Aerts, J. *J. Chem. Res.* **1985**, *388*, 4201.

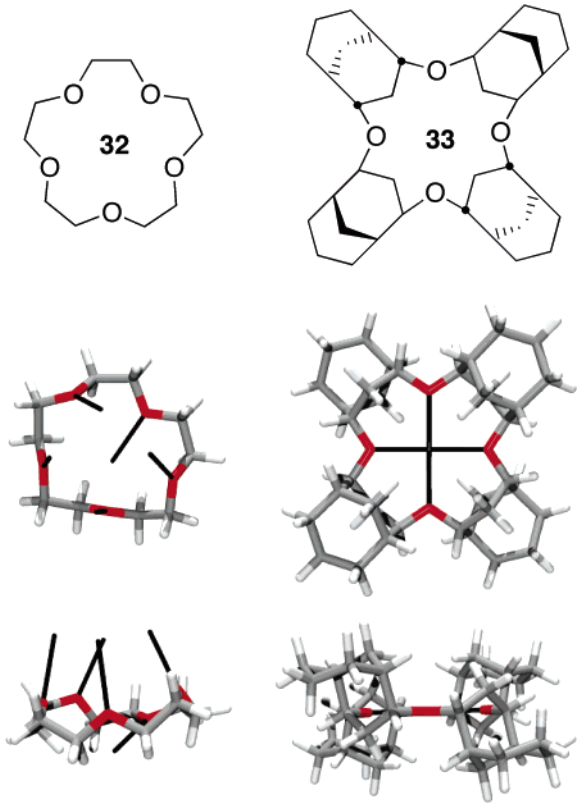

Figure 14. MM3-optimized geometries for the Na^+ binding conformations of **32** and **33**. The 2.5 Å vectors attached to each oxygen atom depict the dipole moment for each ether group.

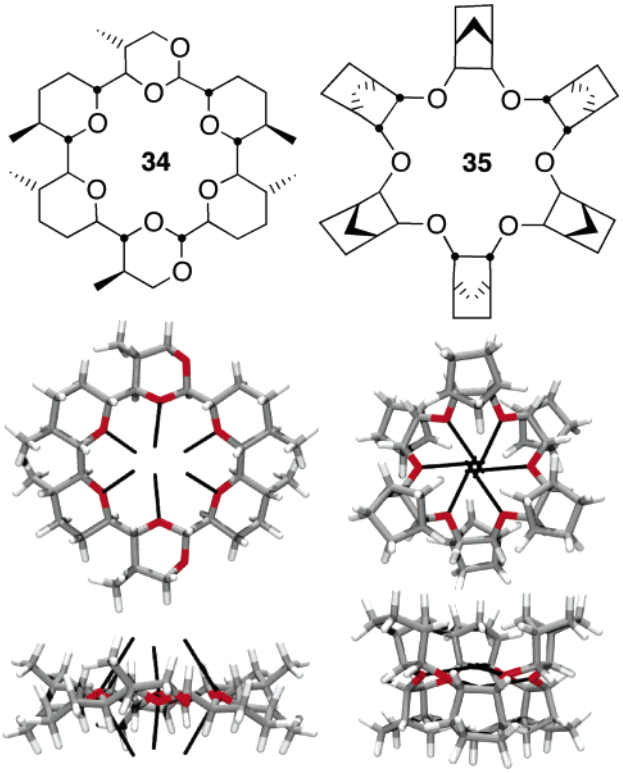

Figure 15. MM3-optimized geometries for the K^+ binding conformations of **34** and **35**. The 3.0 Å vectors attached to each oxygen atom depict the dipole moment for each ether group.

rocycle, **33**, assembled from building block **22** (Figure 11). The Na^+ binding conformation[25] of the flexible **32** is compared with that of the preorganized **33** in Figure 14. Visual inspection reveals that **32** fails to provide a complementary dipole orientation whereas **33** offers a highly complementary arrangement. As in the first example, these differences are reflected by ΔU_2 values of 9.8 kcal mol^{-1} for **32** versus 0.2 kcal mol^{-1} for **33**, indicating that **33** is better organized for cation binding. ΔE_2 values of -91.1 kcal mol^{-1} for **32** versus -94.5 kcal mol^{-1} for **33** establish that this is an instance where a highly organized tetradentate ether provides a larger binding affinity than a poorly organized pentadentate ether.

In final example, we consider the complexation of K^+ by two 18-crown-6 macrocycles, the known host **34** and the theoretical host **35** assembled from building block **16** (Figure 10). The motivation for the design of **34** was to preorganize the flexible 18-crown-6 in the D_{3d} binding conformation by appending rings, and conformational analysis confirmed **34** to be locked in the desired conformation.[26] Host **35** is also preorganized. Yet, evaluation of the conformations of **34** and **35** (Figure 15) reveals a significant difference in the organization of the binding sites within these rigid architectures. With three dipoles converging above and three dipoles converging below the cavity, **34** suffers from a lack of complementarity similar to that exhibited by 18-crown-6 (see Figure 2). In contrast, **35** has dipole moments that are directed within the cavity. Once again these differences are reflected in ΔU_2 values of 8.1 kcal mol^{-1} for **34** versus 2.0 kcal mol^{-1} for **35**, and a substantial increase in K^+ binding affinity is established by ΔE_2 values of -60.7 kcal mol^{-1} for **34** versus -82.0 kcal mol^{-1} for **35**.

The examples given above demonstrate that cation binding affinity can be enhanced significantly when multidentate hosts are constructed from organized building blocks. While the three hosts **31**, **33**, and **35** all exhibit dipole moments that converge within the cavity, we note that there are other combinations of the building blocks shown in Figures 10 and 11 that fail to accomplish this feat. Thus, use of organized building blocks is a necessary, but not sufficient, requirement for achieving an organized multidentate host. As a result, proposed assemblies of building blocks must be evaluated for complementarity and preorganization on an individual basis.

Summary

This paper presents a strategy for the deliberate design of improved host architectures. The approach is based on optimal molecular geometries for the interactions between individual host binding sites and the guest. Such information, which can be obtained through either theoretical methods or examination of crystal structure data, provides the basis for identifying structural elements that are able to organize two host binding sites for effective interaction with the guest. When organized structural elements are used as building blocks for multidentate hosts, desirable geometric features are retained leading to stronger binding interactions with the guest.

The identification of the most favorable building blocks is facilitated through the application of novel computer-aided design software. The HD program rapidly searches a large area of structural space and produces a list of top candidates, using geometry to rank them with respect to how well they complement the guest. When it is interfaced with the GMMX program,

(25) Paulsen, M. D.; Hay, B. P. *J. Mol. Struct. (THEOCHEM)* **1998**, *429*, 49.
(26) Li, G.; Still, W. C. *J. Am. Chem. Soc.* **1993**, *115*, 3804.

subsequent evaluation of these candidates using force field-based scoring methods locates structures with desirable properties that include (a) low levels of induced strain on guest complexation, (b) low conformational energy, and (c) minimal number of restricted bond rotations on guest complexation.

The efficacy of these computational methods has been illustrated by a search for improved building blocks for cation hosts containing aliphatic ether oxygen donor groups. A number of structural elements were identified that provide better binding site organization than that offered by the prototypical ethylene linkage. Several examples establish that considerable enhancement in cation binding affinities can be achieved when macrocyclic ethers are assembled from organized structural elements.

Finally, we note that the methods presented herein are general and, with recent modifications to the HD program that allow the treatment of multiatom guests,[14a] these methods have potential application to a wide variety of other host−guest systems.

Acknowledgment. This research was supported by the Environmental Management Science Program (Grant 73759), Office of Science, U.S. Department of Energy (DOE), and performed at Pacific Northwest National Laboratory, managed for DOE by Battelle. RHF calculations were performed using the Molecular Science Computing Facility (MSCF) in the William R. Wiley Environmental Molecular Sciences Laboratory, a national scientific user facility sponsored by the DOE's Office of Biological and Environmental Research and located at PNNL.

Supporting Information Available: Complete ref 20, HostDesigner input files, and Cartesian coordinates and absolute energies for **30**−**35** and their cation complexes. This material is available free of charge via the Internet at http://pubs.acs.org.

JA055169X